Available at www.sciencedirect.com
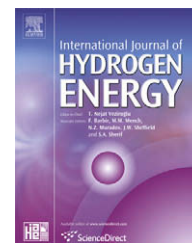
ScienceDirect

journal homepage: www.elsevier.com/locate/he

Comparison criteria for large-scale hydrogen liquefaction processes

David O. Berstad[*], **Jacob H. Stang**[1], **Petter Nekså**[2]

SINTEF Energy Research, Sem Saelands vei 11, NO-7465 Trondheim, Norway

A B S T R A C T

In a hydrogen liquefier the pre-compression of feed gas has generally higher stand-alone exergy efficiency than the cooling and liquefaction sub-process. Direct comparison of liquefiers based on overall exergy efficiency and specific power consumption will favour those with a higher portion of pre-compression. A methodology for comparing hydrogen liquefaction processes that compensates for non-uniformity in feed specifications has been developed and applied to three different hydrogen liquefiers. The processes in consideration have been modified to have equal hydrogen feed pressure, resulting in a more consistent comparison. Decreased feed pressure results in generally higher power consumption but also higher exergy efficiency, and vice versa. This approach can be adapted to the boundary conditions that the liquefaction process will be subject to in a real energy system.

© 2008 International Association for Hydrogen Energy. Published by Elsevier Ltd. All rights reserved.

1. Introduction

The prospect of hydrogen as a significant component in the future energy portfolio is growing. The European Union regards hydrogen as an essential element in low-emission utilisation of fossil energy resources and is setting precedent by funding several extensive R&D projects, many of which involve hydrogen as energy carrier in the supply chain. Throughout the world, hydrogen pilot plants are emerging.

For both centralised energy conversion such as gas-fired power plants and de-centralised, for instance, mobile fuel cells and combustion engines, hydrogen represents techno-logical solutions for pre-combustion CO_2 capture. In the case of de-centralised use, hydrogen must be distributed from central production facilities to intermediate end-user storages. Due to its higher energy density, liquid hydrogen (LH$_2$) may be the preferred option for bulk transport provided that energy-efficient liquefaction processes will be available. LH$_2$ provides flexibility on the retail site as it with little effort can be transformed into any desired form on-site: liquid; gas; supercritical state.

The competitiveness of LH$_2$ as an alternative for distribution is demonstrated by Kramer et al. [1]. In this comprehensive case study on large-scale H$_2$ production and distribution for automotive use, the well-to-wheel cost for LH$_2$ and compressed gaseous hydrogen (CGH$_2$) are close to identical, given a retail-side delivery pressure of 350 bar. However, with integration of LNG evaporation in the liquefaction process, LH$_2$ would become the more economical solution due to decreased manufacturing cost. Further it is

estimated that this energy supply chain may reduce well-to-wheel emissions by up to 85% compared to conventional gasoline and diesel.

Due to high capital and energy cost it is vital for the overall supply chain performance that efficient liquefaction processes are developed. In the efforts for more efficient LH_2 processes, comparison with current state of the art is important for the assessment of new concepts. However, direct comparison of specific power consumption does not provide an objective criterion unless feed and product specifications are uniform. Commonly, these specifications are assumed differently, and in order to obtain consistent comparison criteria the level of abstraction regarding efficiency must be lowered.

The purpose of this work is hence to develop and apply comparison criteria with a higher degree of objectivity for LH_2 processes. In addition, it will provide insight to how feed and product specifications to a certain extent restrict the obtainable efficiency for liquefaction processes.

The next section provides a brief background on LH_2, followed by a methodology section in which comparison criteria are derived from an illustrative theoretical example. Subsequently, one existing and two conceptual liquefaction processes are presented and compared according to the derived comparison criteria.

2. Properties of liquid hydrogen

2.1. Energy density

For bulk distribution of hydrogen to de-centralised gas stations and storages, energy density is a significant factor for the transport economy and thus the overall economy of the supply chain. A comparison of various transportation states shows that LH_2 at 0.1 MPa (1 bar) contains about four times the energy per volume unit than does CGH_2 at 25 MPa (250 bar) and almost three times as much than for 35 MPa (350 bar) [2].

2.2. Liquefaction power

Hydrogen liquefaction requires considerable amounts of energy. Assuming atmospheric pressure for both the H_2 feed and LH_2 product as saturated liquid, specific liquefaction power as function of the exergy efficiency of the process is plotted in Fig. 1. To illustrate the high requisite power, the upper and lower dashed lines indicate LHV and minimum theoretical liquefaction power of H_2, respectively. As can be observed, 40% efficiency or higher is required to obtain specific power lower than an equivalent of 30% of LHV_{H2}. For comparison, the corresponding figure for LNG is 5–6% of LHV_{NG} at 40% process efficiency. As only a fraction of the exergy contained in LH_2 can be recovered in the end-user re-evaporation, it is crucial for the viability of the H_2 energy chain that efficient hydrogen liquefaction technology is developed. It is important to note that LHV is not an exergy-based property but in this case used as a reference for specific liquefaction power.

Minimum theoretical liquefaction power of H_2 is a function of various parameters. The importance of taking into account the available feed pressure for LH_2 processes is illustrated by Quack [3]. Fig. 2 shows the specific exergy content for normal-hydrogen at constant temperature 300 K as function of pressure. As can be observed, a feed stream at 40 bar pressure contains 1.28 kWh/kg_{LH2} exergy and would thus reduce w_{min} from Fig. 1 by 32%.

Besides pressure, temperature and ambient conditions, the liquid-product exergy content is also dependent on the composition of ortho- and para-hydrogen. Given a feed stream of normal-H_2 at ambient state 1.0 bar and 300 K, the minimum specific power required to obtain saturated liquid at 1.0 bar and equilibrious ortho-para composition, equals 3.94 kWh/kgLH2 [3]. The contribution from conversion of ortho- to para-H_2 corresponds to 0.59 kWh/kg_{LH2} or about 15% of the total reversible work. Due to an otherwise unacceptable boil-off rate, commercial LH_2 production normally operates with a product para fraction of at least 95%. In the higher end Quack proposes equilibrium composition for saturated liquid at 1.0 bar, corresponding to a para content of 99.8%.
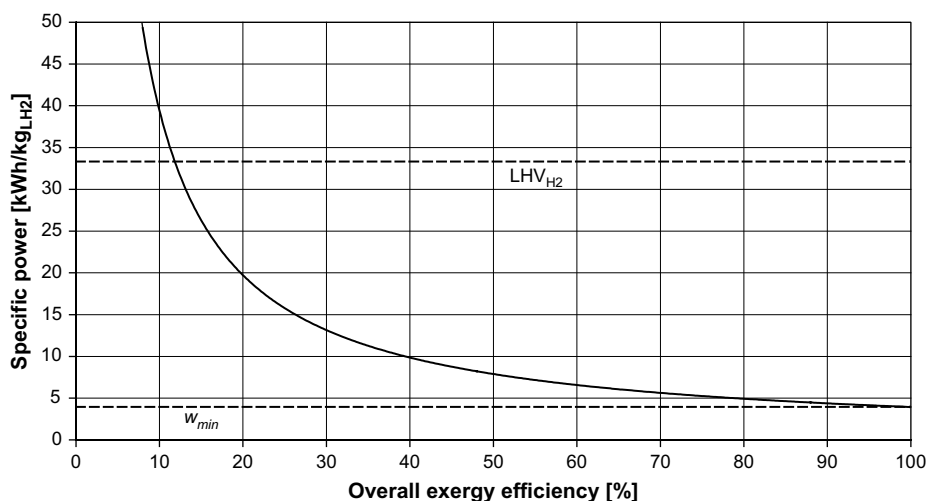

Fig. 1 – Specific power consumption as function of overall exergy efficiency for liquefaction of H_2 from gaseous feed at 1.0 bar to saturated liquid at 1.0 bar.
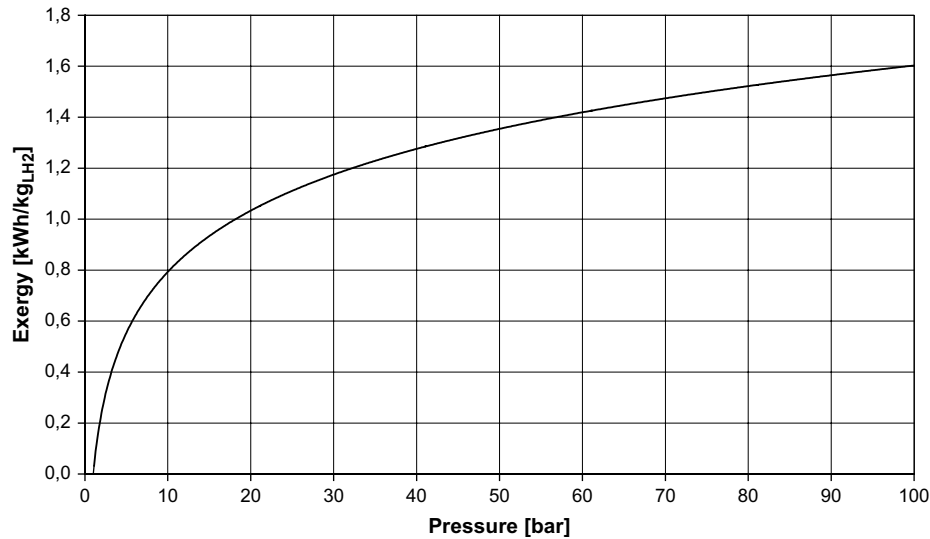
Fig. 2 – Specific exergy diagram for normal-hydrogen at 300 K as function of pressure. Ambient conditions: T_0 = 300 K and P_0 = 1.0 bar assumed.

Although the conversion from normal-H_2 to a very high fraction of para-H_2 accounts for a significant portion of the LH_2 exergy content, variation of the product para fraction within the interval 95.0–99.8% has relatively little effect compared to changes in, for instance, feed pressure. This is exemplified in Table 1 where the absolute change in minimum specific liquefaction power $|\Delta w_{min}|$ is calculated with respect to changes in parameters affecting the reversible work. For each parameter an interval is defined in which it may vary depending on process design and location. From the results it can be observed that given the defined intervals, minimum specific liquefaction power is more sensitive to feed pressure and less to para-H_2 content. Furthermore, it shows that variation in ambient temperature has potentially greater impact than liquid-product saturation pressure.

2.3. Thermodynamic properties

Throughout this work thermodynamic properties for normal- and para-H_2 have been retrieved from tabular data from the NIST Reference Fluid Thermodynamic and Transport Properties Database (REFPROP). The specific exergy difference Δe between two arbitrary states is calculated by

$$e_2 - e_1 = h_2 - h_1 - T_0(s_2 - s_1) \qquad (1)$$

where h and s denote specific enthalpy and entropy, respectively.

For feed streams, difference in exergy is calculated based on thermodynamic properties for normal-H_2. This is accurate for a wide temperature interval as the composition of ortho- and para-H_2 remains close to constant for higher temperatures. To illustrate this, the equilibrious ortho-H_2 fraction at 300 and 250 K differ by about 0.2% units only. Correspondingly, tabular data for pure para-H_2 is applied in calculations of exergy difference between various liquid-product states. Calculations for ortho-para conversion exergy are based on tabular data for equilibrious ortho-para composition and heat of conversion by Woolley et al. [4].

In this work the term ''normal-hydrogen'' solely refers to the equilibrium composition at ambient temperature, i.e. 75 mole-% ortho-H_2 and 25 mole-% para-H_2.

3. Methodology – conception of efficiency and comparison criteria

Numerous reports in published literature refer to and compare hydrogen liquefaction plant performances with respect to specific power consumption and frequently emphasise this as the primary key figure of interest. This is done, for instance, by Bossel et al. [5,6]. Although this figure does provide information on the actual power consumption within individually defined system boundaries it does not necessarily apply as basis for comparison between processes.

Furthermore, various definitions of process efficiency can be observed, some of which view energy units of power and heat equally in formulas as done by Schwartz [7]. Hence, a reported efficiency figure is basically irrelevant as information unless its exact definition is known.

In this work the exergy efficiency η_{ex} for a liquefaction process is defined as the ratio between increased exergy

Table 1 – Sensitivity of minimum specific liquefaction power subject to changes in process parameters within defined intervals.

Parameter	Interval	$\|\Delta w_{min}\|$ [kWh/kg_{LH2}]	Relative change [%]
LH_2 para fraction [%]	95.0–99.8	0.09	2
H_2 feed pressure [bar]	1.0–60	1.42	36
LH_2 saturated pressure [bar]	1.0–4.0	0.22	6
Ambient temperature [K]	283–303	0.32	8

Relative change is defined as absolute change divided by 3.94 kWh/kg_{LH2}.

content of H_2 between feed and product state, and the net amount of power consumed in the process:

$$\eta_{ex} = \frac{e_{product} - e_{feed}}{w_{net}} \qquad (2)$$

Increase in exergy content is calculated from Eq. (1) while net specific power equals the net sum of all power crossing the system boundaries. From the viewpoint of exergy utilisation this is a very useful definition as it provides the ratio between the ideal reversible work required to liquefy the H_2 feed and the actual work consumed in the process. This efficiency criterion is referred to as rational efficiency by Kotas [8] and can also be applied to sub-processes within the boundaries of the liquefaction process.

Direct comparison between different H_2 liquefaction plants with respect to efficiency or specific power is in many cases not justified, as operating conditions are not uniform. Feed and liquid-product conditions do vary and efficiency calculations may therefore not be based on equal premises. To illustrate this point, Fig. 3 shows the general flow diagram of a process in which the H_2 feed is first pre-compressed, then liquefied in a black-box process and extracted as liquid-product. Two different system boundaries are defined: (A) including pre-compression; and (B) excluding pre-compression. Three state points for H_2 are indicated: (1) upstream of pre-compression; (2) downstream of pre-compression; and (3) as LH_2 product.

Furthermore, two arbitrary processes I and II both deliver LH_2 as saturated liquid at 1.0 bar but differ as they are supplied with hydrogen at different pressure levels. Feed pressure for processes I and II equals 1.0 and 20 bar, respectively. System boundaries A now embody process I with feed state (1) while boundaries B and feed state (2) apply for process II. Furthermore, due to identical black-box liquefaction processes, the feed of process I must be compressed to 20 bar while no compression is required for process II. Exergy efficiency figures for the pre-compression and liquefaction sub-process are given by Eqs. (3) and (4), respectively.

$$\eta_{ex,PC} = \frac{e_2 - e_1}{w_{PC}} \qquad (3)$$

$$\eta_{ex,L} = \frac{e_3 - e_2}{w_L} \qquad (4)$$

Combining Eqs. (2), (3) and (4) the resulting overall process exergy efficiency equals the weighted average of the two sub-process efficiencies based on their respective contributions to the net power consumption:

$$\eta_{ex} = \eta_{ex,PC}\frac{w_{PC}}{w_{PC} + w_L} + \eta_{ex,L}\frac{w_L}{w_{PC} + w_L} \qquad (5)$$

With an assumed exergy efficiency of 35% for the black-box liquefaction process and 70% for pre-compression, process parameters and calculated results are summarised in Table 2.

From the results it can be observed that process I is the more exergy efficient even though it is consuming more power and operating with an identical black-box liquefaction process. The explanation for the lower exergy efficiency of process II lies in the exergy increase of H_2 which is comparably smaller due to higher feed pressure. As can be observed in Fig. 2, a feed stream supplied at 20 bar contains 1.03 kWh/kg of exergy, more than 25% of the exergy content of saturated liquid at atmospheric pressure. Hence, considering specific power the yardstick for performance and quality of LH_2 processes is incorrect unless both feed and product specifications are uniform.

Given constant $\eta_{ex,PC} = 70\%$ the overall exergy efficiency η_{ex} for processes I and II is plotted as function of $\eta_{ex,L}$ in Fig. 4. From Eq. (5) it is obvious that in case of identical values for $\eta_{ex,PC}$ and $\eta_{ex,L}$, the overall efficiency η_{ex} also becomes equal to these. This can be observed as the curves for processes I and II reach common function value in the special case of $\eta_{ex,PC} = \eta_{ex,L} = 70\%$.

4.   State-of-the-art liquefaction plants

In the assessment of new concepts for hydrogen liquefaction they should be thoroughly compared with the performance of existing large-scale LH_2 plants. From published literature, best state-of-the-art performance regarding power consumption is found to be in the range 10–15 kWh/kg$_{LH2}$. In the lower end, Quack [9] refers to Kinnard [10] when stating 10 kWh/kg$_{LH2}$ as best performance of LH_2 plants in the United States. Kinnard, however, reports plant capacities with no corresponding figures for power consumption disclosed, thus leaving this number unconfirmed. In the higher end there is well-documented and
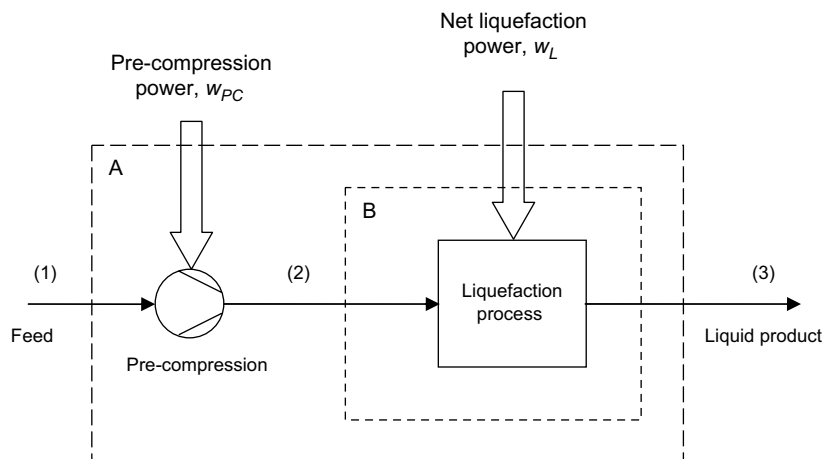

Fig. 3 – General process flow diagram for hydrogen liquefaction.

Table 2 – Process parameters and results.

	Process I	Process II
Feed stream state	(1)	(2)
Feed pressure [bar]	1.0	20
Feed temperature [K]	300	300
LH$_2$ product stream state	(3)	(3)
LH$_2$ product pressure [bar]	1.0 (sat. liquid)	1.0 (sat. liquid)
$\eta_{ex,PC}$ [%]	70.0	N/A
$\eta_{ex,L}$ [%]	35.0	35.0
$e_{product} - e_{feed}$ [kWh/kg$_{LH2}$]	3.94[a]	2.91[a]
w_{PC} [kWh/kg$_{LH2}$]	1.48	0
w_L [kWh/kg$_{LH2}$]	8.32	8.32
w_{net} [kWh/kg$_{LH2}$]	9.79	8.32
η_{ex} [%]	40.3	35.0

a 99.8% para content for state (3) and ambient conditions $T_0 = 300$ K and $P_0 = 1.0$ bar assumed.

available information on the Ingolstadt plant [11,12]. With the lack of available detailed information on the US LH$_2$ plants it cannot be concluded that a liquefaction plant in the 10 kWh/kg$_{LH2}$ range is more exergy efficient than, for instance, Ingolstadt, despite lower specific power consumption.

Different sources claim an Ingolstadt specific power consumption of 13.6 [11,12], 13 [13] and 15 kWh/kg$_{LH2}$ [9], respectively. A possible explanation for this discrepancy may be differing assumptions for the specific production power of LN$_2$, applied in open-cycle pre-cooling in the process.

The above examples of information scarcity and deviation illustrate the difficulty in the work of performing consistent comparisons of H$_2$ liquefaction processes.

4.1. The Ingolstadt LH$_2$ plant

Liquid hydrogen at 1.3 bar with a para content of at least 95% is delivered by the Ingolstadt plant at a production rate of

approximately 4.4 t/d. The state of the feed stream is 21 bar and <308 K. An open nitrogen cycle provides pre-cooling while a Claude cycle generates the further cooling and throttling required in order to obtain the liquid-product. Process flow diagram and further details on the process are reported by Gross et al. [11] and Bracha et al. [12].

A thermodynamic efficiency of 33% is reported "with respect to an ideal Carnot cycle with four-stage ortho-para conversion." It is here presumed that the irreversibilities occurring in the stepwise ortho-para conversion are regarded inevitable and thus not considered. However, as there has been development towards continuous conversion with less intrinsic irreversibility the ortho-para conversion process should still be part of the overall performance analysis. In this notion the exergy efficiency criterion shows robustness as it also comprises this effect.

In order to obtain the exergy efficiency as defined in this work the feed-to-product exergy increase is calculated in Fig. 5, solely based on the feed and liquid-product states. Due to high pressure the H$_2$ feed already contains a considerable amount of exergy, reducing the total exergy increase. The calculation shows 27.5% reduction in minimum theoretical power compared to the case of feed and product specifications both at 1.0 bar. Ambient temperature $T_0 = 300$ K and equilibrious product para-H$_2$ fraction are assumed. Total specific liquefaction energy, presumably power, of 0.950 kWh/l$_{LH2}$ is reported. With a liquid density of 69.8 kg/m^3 for para-H$_2$ at 1.3 bar corresponds to 13.6 kWh/kg$_{LH2}$. The exergy efficiency calculation is shown in Table 3.

5. New concepts for hydrogen liquefaction

Extensive infrastructure for production, storage and distribution is a prerequisite for H$_2$ to become a significant energy carrier in the energy portfolio. For a larger metropolitan area with 100,000–200,000 hydrogen vehicles the automotive consumption rate will be in the magnitude of 100 t/d [1].
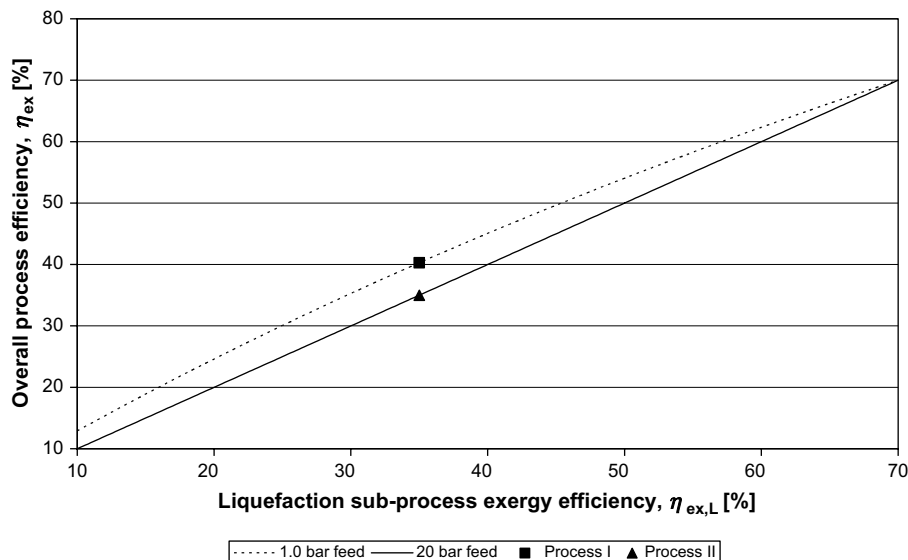

Fig. 4 – Overall exergy efficiency for the generic LH$_2$ processes as function of exergy efficiency of the liquefaction sub-process. Constant pre-compression efficiency of 70% is assumed.
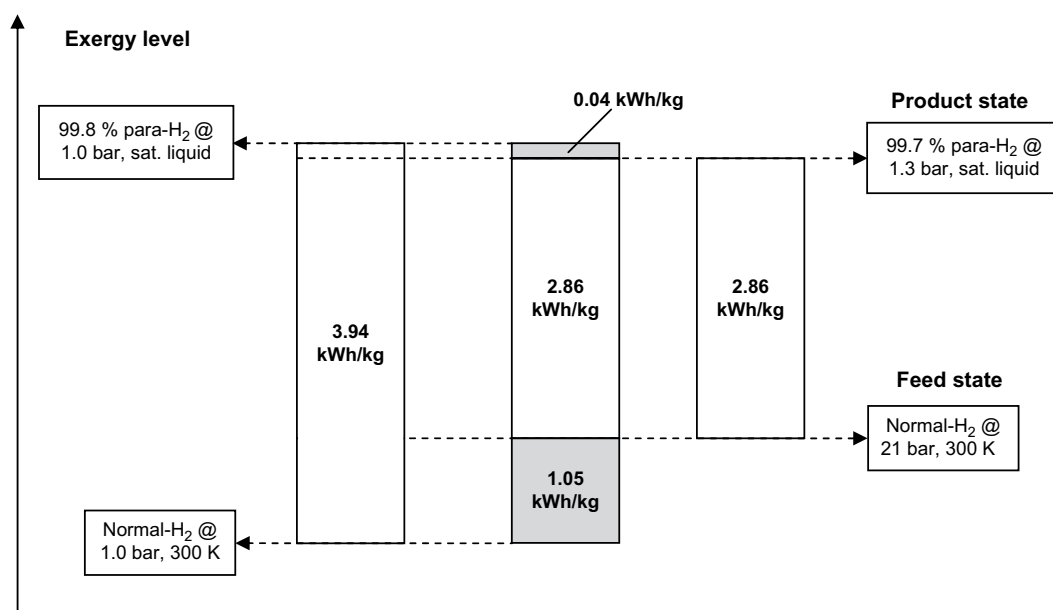
Fig. 5 – Calculation of feed-to-product exergy increase for the Ingolstadt process.

Comparing this with, for instance, the 4.4 t/d production rate in Ingolstadt, it is obvious that considerably larger plants would be needed within this scenario. Hence, large production rates and high efficiency would be desired characteristics for future LH$_2$ plants. This section presents two proposed concepts showing prospect of lower power consumption and higher efficiency than state of the art. These are the hydrogen liquefaction processes proposed by Quack [3] and the World Energy NETwork (WE-NET) project [14]. In addition, a high-efficiency large-scale LH$_2$ process has been developed by Valenti and Macchi [15]. The latter, with an 800–900 t/d liquefaction rate, has a reported exergy efficiency and specific power of 47.7% and 5.04 kWh/kg$_{LH2}$, respectively. This process will not be further evaluated here but is highly relevant in the development of efficient large-scale LH$_2$ processes.

5.1. The LH$_2$ process proposed by Quack

Quack's concept is not fixed at a certain production rate, however, large-scale operation in the magnitude of 170 t/d is indicated. H$_2$ feed is first compressed from 1.0 to 80 bar in five stages. A combination of ambient and propane inter-cooling takes place after each stage. At 80 bar pressure the H$_2$ stream is cooled to 220 K by a three-stage propane refrigeration cycle. An objection to this process design is the low-pressure propane refrigeration stage. For pure propane providing cooling at an evaporation temperature of 217 K, the corresponding evaporation gauge pressure becomes negative, which in refrigeration process design is a generally undesirable parameter.

Furthermore, the high-pressure stream of H$_2$ is cooled to approximately 25 K by an inverted two-stage Brayton cycle employing helium with 20 mole-% neon content as refrigerant. The final liquefaction is obtained by expansion from supercritical state at 80 bar into two-phased state at 1.0 bar in a rotating liquid expander. The flash gas fraction, equal to

8.9% of the product stream, is separated from the LH$_2$ product. This recycle stream is then re-compressed to 8.0 bar, sub-cooled and subsequently re-liquefied by a Joule–Thompson expansion.

Continuous equilibrium ortho-para conversion is taking place during the cooling process, as catalysts are assumed to be packed inside the hydrogen side of the heat exchangers. This concept, given its inherent assumptions, shows promising figures with specific power consumption in the range 7–8 kWh/kg$_{LH2}$. Further details on the process are documented by Quack [3].

5.2. The WE-NET LH$_2$ process

One of the concepts developed by the WE-NET project is a 300 t/d large-scale process delivering LH$_2$ at 1.06 bar from a feed stream of equal pressure. Similarly to the Quack process, the H$_2$ feed is compressed to approximately 50 bar prior to pre- and sub-cooling. A closed nitrogen refrigeration cycle provides pre-cooling to about 80 K while further sub-cooling is generated by a hydrogen Claude cycle.

At low temperature the main process stream of H$_2$ is expanded in a supercritical low-temperature expander to an intermediate pressure level, but unlike the Quack process, no vapour is tolerated. Further sub-cooling takes place before the stream of H$_2$ is partially liquefied by a Joule–Thompson expansion. The flash gas is then internally heat-exchanged and recycled to the feed gas compressor.

Table 3 – Data for exergy calculation for the Ingolstadt LH$_2$ process.	
Minimum theoretical liquefaction power [kWh/kg$_{LH2}$]	2.86
Net specific power [kWh/kg$_{LH2}$]	13.6
Exergy efficiency [%]	21.0

Table 4 – Assumptions for the Quack and WE-NET concepts.

	Quack	WE-NET
Liquefaction capacity [t/d]	170	300
H_2 feed pressure [bar]	1.0	1.06
LH_2 product pressure [bar]	1.0	1.06
Para-hydrogen fraction, LH_2 product [%]	>99	>95
Efficiency, main compressors [%]	85 (isentropic)	80[a]
Efficiency, main expanders [%]	90 (isentropic)	85[a]
Power recovery efficiency, expanders [%]	98	90
Motor efficiency, large/small units [%]	96/80	Unknown
Efficiency, cold H_2 expander [%]	85 (isentropic)	85[a]
Vapour fraction, cold H_2 expander [%]	~9	0[b]
Minimum internal temperature approach [K]	1.33	N/A
Pressure drop in HX	Unknown	None
Cold-box heat leak	None	None
Ortho-para conversion	Continuous	Partially continuous
Storage tank capacity [m^3]	N/A	50,000
Hydrogen evaporation rate [%/d]	N/A	0.1

a Efficiency category not declared.
b 100% supercritical with liquid density.

Ortho-para conversion in this process is a combination of continuous and non-continuous. The non-continuous part occurs at approximately 80 K as a conversion to 47% para-H_2 takes place in a nitrogen-cooled converter. For the remainder, continuous conversion is assumed.

As for the Quack process, the power requirement is less than for the Ingolstadt reference plant, with a specific liquefaction power calculated to 8.5 kWh/kg$_{LH2}$. More details on the WE-NET process can be found in the work by Matsuda and Nagami [14].

5.3. Comparison of the Quack and WE-NET processes

Quack and WE-NET operate with virtually uniform H_2 feed and product specifications and can be compared directly with a relative error margin in the magnitude 0.1–1% regarding exergy if uniform para-H_2 fraction is assumed. Other assumptions do differ, however, for instance, compressor and expander efficiencies. The most important figures for each process are disclosed in Table 4 while overall process calculations are performed in Tables 5 and 6.

Table 5 – Quack process calculation results.

H_2 (compression minus recovered expansion) [kWh/kg$_{LH2}$]	1.97
Propane compression [kWh/kg$_{LH2}$]	0.18
He/Ne (compression minus recovered expansion) [kWh/kg$_{LH2}$]	4.35
Total [kWh/kg$_{LH2}$]	6.50
Estimated auxiliary mark-up [kWh/kg$_{LH2}$]	0.43
Estimated net power [kWh/kg$_{LH2}$]	6.93
Minimum theoretical liquefaction power [kWh/kg$_{LH2}$]	3.94
Exergy efficiency [%]	56.8

Table 6 – WE-NET process calculation results.

H_2 compression [kWh/kg$_{LH2}$]	6.00
N_2 compression [kWh/kg$_{LH2}$]	2.81
Total [kWh/kg$_{LH2}$]	8.80
Recovered expansion power [kWh/kg$_{LH2}$]	0.27
Net power [kWh/kg$_{LH2}$]	8.53
Minimum theoretical liquefaction power [kWh/kg$_{LH2}$]	3.94[a]
Exergy efficiency [%]	46.2[b]

a For simplicity, feed-to-product exergy increase equal to that of the Quack process is assumed.
b 0.2% unit deviation from WE-NET source [14].

6. Consistent comparison of Quack and WE-NET with Ingolstadt

Calculated exergy efficiencies, the ratio between feed-to-product exergy increase and net power consumption, are now available for all three processes. With 56.8 and 46.2 versus 21.0%, the new concepts show significantly higher efficiency than Ingolstadt. Due to levels of abstraction in the available reports, detailed exergy analyses have not been performed, excluding a complete overview of individual sources of irreversibility for the processes.

Since H_2 is commonly generated at relatively high pressure in chemical reforming processes and electrolysers, higher feed pressure for Quack and WE-NET are realistic scenarios for an extended analysis. When assuming H_2 feed pressure equal to that of Ingolstadt but otherwise unchanged liquefaction processes, it is obvious that the specific power consumption will decrease as a consequence of lower pre-compression power. Calculations for this modification of Quack and WE-NET are shown in Table 7. A pre-compression exergy efficiency of 73% is reported by Quack [3] and correspondingly 68.7% is applied for WE-NET, based on an equal-ratio assumption between the compressor efficiencies in Table 4 and resulting exergy efficiencies. Alternatively, the Ingolstadt feed pressure can be reduced to 1.0 bar with a back-calculated penalty for power of compression to 21 bar. Calculation for this modification is shown in Table 8.

From the graphical representation in Fig. 6, the effect of simultaneously decreasing exergy efficiency and power consumption can be observed for Quack and WE-NET. For the

Table 7 – Calculation of specific power consumption and exergy efficiency for Quack and WE-NET when H_2 feed pressure increases from 1.0 to 21 bar.

	Quack	WE-NET
Net power, original process [kWh/kg$_{LH2}$]	6.93	8.53
H_2 feed exergy increase [kWh/kg$_{LH2}$]	1.05	1.05
H_2 compression power reduction [kWh/kg$_{LH2}$]	1.44[a]	1.53[b]
Net power, modified process [kWh/kg$_{LH2}$]	5.49	7.00
Minimum theoretical liquefaction power [kWh/kg$_{LH2}$]	2.89	2.89
Exergy efficiency, modified process [%]	52.6	41.3

a Compression exergy efficiency assumption of 73%.
b Compression exergy efficiency assumption of 68.7%.

Table 8 – Specific power and exergy efficiency for the Ingolstadt process when H_2 feed pressure is reduced from 21 to 1.0 bar.	
Net power, original process [kWh/kg$_{LH2}$]	13.6
H_2 feed exergy reduction [kWh/kg$_{LH2}$]	1.05
H_2 compression power increase [kWh/kg$_{LH2}$]	1.50[a]
Net power, modified process [kWh/kg$_{LH2}$]	15.1
Minimum theoretical liquefaction power [kWh/kg$_{LH2}$]	3.91
Exergy efficiency, modified process [%]	25.9
a Compression exergy efficiency assumption of 70%.	

modified Ingolstadt process the opposite is the case as both specific power and exergy efficiency increase. These effects are caused by changes in contribution from the compression sub-process to the overall exergy efficiency, analogously to the illustrative example presented earlier.

The modified Quack and WE-NET models operate with feed and product specifications close to those of Ingolstadt. Hence, a basis for comparison with higher degree of objectivity is obtained as they have become more similar with regard to boundary conditions. This is graphically illustrated by the alignment of points of operation along the lines representing the relation between overall exergy efficiency and specific power for fixed sets of feed and product specifications, denoted ''iso-curves'' in this work.

7.   Discussion

From the calculated changes in minimum theoretical liquefaction power occurring over the various intervals defined in Table 1, feed pressure is clearly the most potent source of deviance of this parameter between different LH$_2$ processes. Hence, and due to the fact that efficiency of pre-compression is considerably higher than for cooling and liquefaction sub-processes, specific power and exergy efficiency will in many cases not provide an objective basis for comparison of

liquefiers. Thus, it is of great importance that processes are compared on equal premises.

The relatively efficient Quack process has generally more advantageous assumptions while those of the relatively inefficient Ingolstadt process are less favourable. Qualitatively, the use of isobaric evaporation of H$_2$ and N$_2$ as cooling in Ingolstadt results in larger heat-transfer irreversibilities than for Quack, as a consequence of larger heat-transfer temperature differences. Furthermore, the high efficiencies for rotating compressors and expanders assumed by Quack give this process a comparative advantage.

For the final step of liquefaction, Quack employs a rotating two-phase expander, which is more efficient than an isenthalpic Joule–Thompson expansion. As Ingolstadt and WE-NET only allow throttling for expansion within the two-phased region, these will be less effective than for Quack. Hence, the Quack process requires less H$_2$ gas recycling than if it did not allow its current two-phase expander.

The entirely continuous and equilibrious ortho-para conversion model in the Quack process has no intrinsic irreversibilities. On the other hand, isothermal conversion reactors in the Ingolstadt and WE-NET processes inevitably result in irreversibilities caused by non-equilibrious ortho-para conversion and thus contribute to lower overall exergy efficiency.

Due to generally lower exergy efficiencies of liquefaction sub-processes than for pre-compression, exclusion of the latter from system boundaries lowers both exergy efficiency and specific power consumption. By assuming H$_2$ feed pressure equal to that of Ingolstadt, specific power for the Quack and WE-NET processes decreases from 6.93 to 5.49 and 8.53 to 7.00 kWh/kg$_{LH2}$, respectively. Exergy efficiencies correspondingly decrease from 56.8 to 52.6 and 46.2 to 41.3%. For Ingolstadt, back-calculation to an envisaged feed pressure of 1.0 bar increases specific power from 13.6 to 15.1 kWh/kg$_{LH2}$ and exergy efficiency from 21.0 to 25.9%.

As both the Quack and WE-NET liquefaction processes are not realised, they should be compared with equal assumptions for parameters in the respective simulation models.
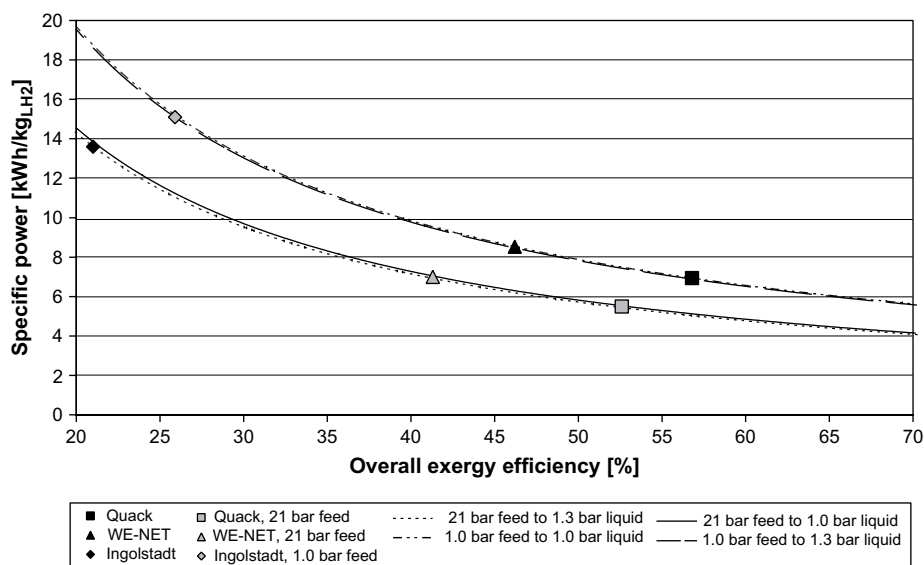

Fig. 6 – Graphical representation of Quack, WE-NET and Ingolstadt on iso-curves. Black and grey markers represent the original and modified processes, respectively.

Examples of parameters to be equalised are ambient conditions; compressor and expander efficiencies; power recovery efficiency; two-phase tolerance in cold H_2 expanders; ortho-para conversion efficiency; minimum temperature approach for heat exchangers.

The methodology described in this work should be further developed and expanded to encompassing justified comparisons of complete well-to-wheel hydrogen distribution chains.

8.   Conclusion

More than a direct calculation of overall exergy efficiency and specific power consumption is required in order to obtain an objective basis for comparison of hydrogen liquefaction processes. As exemplified in this work, also needed is compensation for varying proportions of pre-compression between the processes in consideration. Otherwise a process with a larger portion of pre-compression will show better efficiency than another of similar quality, in which pre-compression contributes less to the overall exergy efficiency. A more justified basis for comparison is therefore the alignment of process characteristics on iso-curves representing the relation between overall exergy efficiency and specific power for fixed sets of feed and product specifications.

Although still in the concept phase, several new designs show significantly improved estimates for power consumption and efficiency from current hydrogen liquefiers. If the demand of liquid hydrogen will increase, allowing the realisation of a new generation of large-scale plants, the margins of efficiency improvement are considerable.

Acknowledgements

REFERENCES

[1] Kramer GJ, Huijsmans JPP, Austgen DM. Clean and green hydrogen. In: 16th World hydrogen energy conference; 2006.

[2] Wolf J. LH_2 makes you mobile. Linde Rep Sci Technol 2003;1: 30–5.

[3] Quack H. Conceptual design of a high efficiency large capacity hydrogen liquefier. Adv Cryog Eng 2001;47:255–63.

[4] Woolley HW, Scott RB, Brickwedde FG. Compilation of thermal properties of hydrogen in its various isotopic and ortho-para modifications. J Res Natl Bur Stand 1948;41:379–475.

[5] Bossel U, Eliasson B, Taylor G. The future of the hydrogen economy: bright or bleak? Cogener Compet Power J 2003; 18(3):29–70 (revised 2005).

[6] Bossel U. Does a hydrogen economy make sense? Proc IEEE 2006;94(10):1826–37.

[7] Schwartz J. Advanced hydrogen liquefaction. NY, USA: Praxair Technology; June 11, 2008. DOE Annual Merit Review Meeting.

[8] Kotas TJ. The exergy method of thermal plant analysis. reprint ed. Melbourne, FL, USA: Krieger Publishing Company; 1995.

[9] Quack H. Die Schlüsselrolle der Kryotechnik in der Wasserstoff-Energiewirtschaft. Kl. Luft- und Kältetechnik 2002;38(3):157–61.

[10] Kinnard GE. The commercial use of liquid hydrogen over the last 40 years. Section 1. In: Proceedings of the 17th international cryogenic engineering conference; 1998. p. 39–44.

[11] Gross R, Otto W, Patzelt A, Wanner M. Liquid hydrogen for Europe – the Linde plant at Ingolstadt. Linde Rep Sci Technol 1994;54:37–43.

[12] Bracha M, Lorenz G, Patzelt A, Wanner M. Large-scale hydrogen liquefaction in Germany. Int J Hydrogen Energy 1994;19(1):53–9.

[13] Weindorf W, Bünger U, Schindler J. Comments on the paper by Baldur Eliasson and Ulf Bossel "The future of the hydrogen economy: bright or bleak?". Ottobrunn: L-B-Systemtechnik GmbH; 2003.

[14] Matsuda H, Nagami N. Study of large hydrogen liquefaction process. Kawasaki City: Nippon Sanso Corp.; 1997.

[15] Valenti G, Macchi E. Proposal of an innovative, high-efficiency, large-scale hydrogen liquefier. Int J Hydrogen Energy 2008;33(12):3116–21.